Reprinted from

dynamics of atmospheres and oceans

planetary fluid, climatic and biogeochemical systems

Dynamics of Atmospheres and Oceans 21 (1994) 53–82

A study of water mass transformation in the Mediterranean Sea: analysis of climatological data and a simple three-box model

Eli Tziperman [a,*], Kevin Speer [b]

[a] *Environmental Sciences and Energy Research, The Weizmann Institute of Science, Rehovot, 76100 Israel*
[b] *Laboratoire de Physique des Océans, IFREMER, B.P. 70, 29280 Plouzané, France*

Received 25 January 1993; revised 10 February 1994; accepted 25 April 1994

ELSEVIER

DYNAMICS OF ATMOSPHERES AND OCEANS

PLANETARY FLUID, CLIMATIC AND BIOGEOCHEMICAL SYSTEMS

Aims and Scope

The journal exists for the publication of research articles on the fluid dynamics of atmospheres and oceans and their interactions, on related basic dynamical processes, and on climatic and biogeochemical problems in which the fluid dynamics play an essential role. Theoretical, numerical, observational and laboratory studies are all welcome.

Publication Information

Dynamics of Atmospheres and Oceans (ISSN 0377-0265). For 1995 volumes 21–22 are scheduled for publication. Subscription prices are available upon request from the publisher. Subscriptions are accepted on a prepaid basis only and are entered on a calendar year basis. Issues are sent by surface mail except to the following countries where Air delivery via SAL mail is ensured: Argentina, Australia, Brazil, Canada, Hong Kong, India, Israel, Japan, Malaysia, Mexico, New Zealand, Pakistan, China, Singapore, South Africa, South Korea, Taiwan, Thailand, USA. For all other countries airmail rates are available upon request. Claims for missing issues must be made within six months of our publication (mailing) date. Please address all your requests regarding orders and subscription queries to: Elsevier Science B.V., Journal Department, P.O. Box 211, 1000 AE Amsterdam, The Netherlands. Tel.: 31-20-4853642, Fax: 31-20-4853598.

Journal Information Center

For further information, or a free sample copy of this or any other Elsevier Science journal, readers in the USA and Canada can contact the following address: Elsevier Science Inc., Journal Information Center, 655 Avenue of the Americas, New York, NY 10010, USA, tel: (212) 633-3750, fax. (212) 633-3784.

ELSEVIER

Dynamics of Atmospheres and Oceans 21 (1994) 53–82

dynamics of atmospheres and oceans

A study of water mass transformation in the Mediterranean Sea: analysis of climatological data and a simple three-box model

Eli Tziperman [a,*], Kevin Speer [b]

[a] *Environmental Sciences and Energy Research, The Weizmann Institute of Science, Rehovot, 76100 Israel*
[b] *Laboratoire de Physique des Océans, IFREMER, B.P. 70, 29280 Plouzané, France*

Received 25 January 1993; revised 10 February 1994; accepted 25 April 1994

Abstract

Upper bounds are estimated for the rates of water mass formation in different regions of the Mediterranean Sea by calculating the monthly climatological air–sea fluxes of heat and fresh water as a function of the surface density. It is found that a yearly averaged flux of about 4 Sverdrup (Sv) of surface water whose density is in the intermediate density range $26.2 > \sigma > 28.7$ is transformed by air–sea fluxes to greater densities, and about 2 Sverdrups are transformed to lesser densities. Part (possibly a small part) of the water transformed into higher density ranges sinks and forms the intermediate and deep water masses. The calculation therefore gives an estimated maximal bound of about 4 Sverdrup for the yearly averaged water mass formation in the Mediterranean. Similar calculations for the Eastern Mediterranean alone give bounds of Levantine Intermediate Water formation (1–1.5 Sv), as well as formation in the Adriatic Sea (1–1.5 Sv). A simple model using three variable-volume boxes to represent a marginal sea under seasonal forcing is used to support the data analysis. The model and the data analysis demonstrate the crucial role of mixing and of the seasonal cycle in shaping the water mass transformation in the Mediterranean Sea.

1. Introduction

This work deals with water mass transformation in the Mediterranean Sea. It has two main objectives: first, to estimate quantitatively the water mass formation and transformation by air–sea fluxes in the Mediterranean Sea using data of the climatological monthly averages of heat fluxes, evaporation, precipitation, and of

* Corresponding author.

SSDI 0377-0265(94)00389-E

surface temperature and salinity; and second, to use a simple three-box model to illuminate the role of mixing in the water mass transformation process as cannot be done using the data alone.

The water mass transformation by air–sea fluxes of heat and freshwater (evaporation, precipitation and river runoff) results in the formation of the deep water of the Mediterranean Sea. The Levantine Intermediate Water (LIW) is believed to form south of Asia Minor, the deep water of the East Mediterranean is formed mostly in the Adriatic Sea, and the deep water of the West Mediterranean is formed in the Gulf of Lion. The high-salinity deep Mediterranean water flowing into the Atlantic Ocean through the Straits of Gibraltar can be traced throughout large parts of the World Ocean. Many studies deal with water mass analysis for the Mediterranean (e.g. Wüst, 1960; see also Malanotte-Rissoli and Hecht (1988) and Hopkins (1988) for reviews of the East and West Mediterranean, respectively), but we still lack reliable estimates of the rate of formation of each of the above water masses.

The formation of dense water is the most obvious result of the air–sea fluxes acting on the oceanic water, and therefore normally receives much attention. However, air–sea fluxes are also responsible for the formation of buoyant water in regions of heating or strong precipitation. This process is no less important than the dense water formation, as it is essential for keeping the oceanic stratification in a steady state.

Water mass transformation is normally studied by calculating the mass, heat, salt and tracer balances for a given volume of water, and thereby estimating the amount of water mass formed or modified within that volume. Using this method, however, it is difficult to separate the effects of air–sea fluxes and interior mixing, both of which affect the distribution of water masses in a given region. The method used here allows the calculation of water mass transformation owing to air–sea fluxes only, distinct from the effects of mixing.

Our calculations are based on Tziperman's (1986) approach, which allows the calculation of the amount of water formed at a given density range by the air–sea fluxes. The approach is an extension of Walin's (1982) work, and was also applied by Speer and Tziperman (1992) to data from the North Atlantic Ocean. An interesting extension of the Mediterranean data analysis presented here was given by Lascaratos (1993).

As climatological flux data such as used in this study are notorious for their poor quality, we make a special effort to discuss and demonstrate the robustness of our results by analyzing two different data sets of air–sea fluxes to calculate the water mass transformation in the Mediterranean Sea. In addition, the various sources of possible errors are discussed in detail, and the sensitivity of our results to various aspects of the calculation is thoroughly examined.

The three-box model study presented here deals with issues that cannot be resolved by the data analysis, thus complementing the data analysis and enhancing our understanding of water mass transformation in the Mediterranean Sea. The model demonstrates why mixing must be invoked to explain the shape of water mass transformation in the Mediterranean Sea.

In the following sections we first briefly present the method of calculation (Section 2), and then apply it to estimate the transformation of Mediterranean water masses by surface fluxes of heat, evaporation and precipitation (Section 3). The three-box model is presented and its results discussed in Section 4, and we conclude in Section 5. The Appendix analyses the possible errors caused by errors in the air–sea fluxes and by various aspects of the data analysis.

2. Method

The idea behind the method presented here is that by calculating the total air–sea buoyancy flux as a function of the density of the surface water rather than as a function of location, it is possible to deduce the amounts of water mass formed or modified in any given density range by these fluxes. A detailed derivation of the expressions relating the surface fluxes to water mass transformation and formation has been given by Tziperman (1986) (see also Walin (1982) and Speer and Tziperman (1992)), and we shall only briefly describe it here.

Let the surface fluxes of heat and freshwater (evaporation minus precipitation) be $\mathscr{H}(z,y,t)$ and $\mathscr{E}(x,y,t)$, respectively. Both are functions of location and time, assumed to vary periodically with the seasonal cycle. Given the temperature and salinity of the surface water $T(x,y,t)$ and $S(x,y,t)$, it is possible to calculate the buoyancy flux $(\alpha/C_p)\mathscr{H}-\rho\beta S\mathscr{E}$ as a function of the surface density, where $\alpha=-\partial\rho/\partial T$ and $\beta=\partial\rho/\partial S$ are the derivatives of the density with respect to temperature and salinity (these are the expansion coefficients up to a factor of one over the density). The total buoyancy flux during 1 year, as a function of the surface density, $F(\rho')$, is found from the above fluxes using the following expression:

$$F(\rho')=\int_{1\text{ year}}\mathrm{d}t\iint_{\text{surface area}}\mathrm{d}x\,\mathrm{d}y\left[\frac{\alpha}{C_p}\mathscr{H}(x,y,t)-\rho\beta S(x,y,t)\mathscr{E}(x,y,t)\right]\times\delta[\rho(x,y,t)-\rho'] \tag{1}$$

The delta function appearing in the integral is zero whenever the surface density is not equal to the density ρ', and therefore samples the surface buoyancy flux only for surface water of density ρ'.

It is not difficult to show (Tziperman, 1986) that $F(\rho')$ is the contribution of air–sea fluxes to the mass flux across the isopycnal surface $\rho=\rho'$, during the entire year. This flux can be of two forms. First, some body of water of density ρ can be made either more dense or less dense by the air–sea fluxes, and move to a different location by actually crossing an isopycnal surface that is fixed in space. Second, a water mass of density ρ can change its density as a result of the flux $F(\rho)$ but remain in place. The cross-isopycnal flux in this case is not across any physical surface fixed in space. In the ocean, the two types of cross-isopycnal flux can simultaneously occur at any given location and time.

The water mass formation by air–sea fluxes in the density range $\rho_1<\rho<\rho_2$ is

equal to the difference between flux entering this range across ρ_1, and the flux leaving this range across ρ_2:

$$\text{mass of water formed in the density range } (\rho_2,\rho_1) = F(\rho_2) - F(\rho_1) \qquad (2)$$

Taking the limit as $\rho_1 \to \rho_2$, the amount of water formed at a density range $(\rho,\rho + d\rho)$, is $M(\rho)d\rho$, where

$$M = dF/d\rho \qquad (3)$$

This procedure for analyzing water mass transformation does not require a knowledge of the volume of water involved in the exchange with the atmosphere, but only of the surface properties of this water. The above expressions give the net water mass formation by air–sea fluxes, distinct from the effects of oceanic mixing which may play an important role in modifying the water mass as soon as it is transformed by air–sea fluxes. The dynamical coupling between the surface fields and the air–sea fluxes is implicit in our calculations. We are using the surface fields and air–sea fluxes to diagnose the water mass transformation while ignoring the dynamics that couple them to each other, as is normal in diagnostic studies.

Finally, it should be noted that the flux denoted here by F is the analog of the derivative with respect to temperature of the thermal forcing function, $Q(T)$, discussed by Walin (1982), whereas $M(\rho)$ is the analog of the second derivative of $Q(T)$.

Errors in the calculation of water mass transformation based on the above ideas may result from the insufficient quality of the air–sea flux data (Bunker and Goldsmith, 1979; Bunker et al., 1982). To examine the effect of these errors on our results, we have applied our method to two different sets of climatological air–sea flux data for the Mediterranean Sea (see the Appendix). Our approach is to try to obtain the most information from the available data, rather than simply give up and not use the data at all.

A second source of error is the lack of data of air–sea fluxes and surface water properties as continuous functions of time, rather than monthly climatological averages. Using (1) with these averages may lead to a wrong estimate of water mass formation, especially because water mass formation events are known to occur during short time intervals during which severe weather conditions occur. The Appendix contains a detailed discussion of the error resulting from the use of climatological flux data, showing that the calculation based on monthly averaged climatological fluxes may still be expected to produce reasonable results.

3. Water mass transformation in the Mediterranean Sea

3.1. Data

The air–sea heat flux data were calculated from ship observations (May, 1983), and are given on a 1° grid and in monthly resolution. The surface temperature and

salinity are from the GDEM (generalized digital environmental model) data set (Davis et al., 1986). In this data set, the temperature and salinity are given on a half-degree resolution grid, sea surface temperature is given at monthly resolution and surface salinity in seasonal resolution. The precipitation data are from Jaeger (1976). They are of monthly temporal resolution and are given every 5° longitude and 2.5° latitude. The heat flux data of May (1983) also contain estimates of the latent heat flux above the Mediterranean, and are used to calculate the evaporation above the Mediterranean.

Before using the data to calculate the water mass transformation, all quantities were linearly interpolated in space to a half-degree resolution grid and the salinity was interpolated in time to a monthly resolution.

Finally, the Mediterranean is normally believed to lose to the atmosphere an amount of heat equivalent to a heat flux of about 5 W m^{-2} on a yearly average. Before using the heat flux data for calculating the water mass transformation of the Mediterranean Sea, we have subtracted a constant heat flux at all locations and months to satisfy the above integral constraint. Additional details are given in the Appendix.

3.2. Calculation

For the data analysis, the time integral over 1 year in (1) is replaced by a sum over 12 months (or only over 3 months of a given season; see below), and the area integral is replaced by a sum over all grid points (Andersson et al., 1982)

$$F(\rho') = \frac{1}{\Delta\rho} \sum_{m=1}^{12} \Delta t \sum_{i,j} \Delta x \Delta y \left[\frac{\alpha}{C_p} \mathscr{H}_{ijm} - \rho\beta S_{ijm} \mathscr{E}_{ijm} \right] \hat{\delta}[\rho_{ijm} - \rho'] \tag{4}$$

The delta function in (1) is replaced here by a boxcar function ($\hat{\delta}$) that is equal to one when the surface density is in the interval $(\rho' - \frac{1}{2}\Delta\rho, \rho' + \frac{1}{2}\Delta\rho)$, and to zero elsewhere. The smaller the density interval $\Delta\rho$ used in the calculation, the better the resolution of $F(\rho)$, but also the noisier the result. Several different values were tried, and finally a satisfactory compromise between resolution and noise was achieved for $\Delta\rho = 0.12$ sigma units (corresponding to dividing the total surface density range $\sigma_\theta = (24, 30)$ into 50 equal density groups). The sensitivity of the results to the choice of $\Delta\rho$ is examined in the Appendix.

3.3. Results

The air–sea driven cross-isopycnal fluxes $F(\rho)$ were calculated for the whole Mediterranean (Fig. 1), for the eastern part (Fig. 2) and western part (Fig. 3), and for the Levantine basin alone (Fig. 4).

Each of Figs. 1–4 shows the averaged cross-isopycnal mass flux obtained by summing air–sea fluxes both for the whole climatological year and for each season separately. The seasonal cross-isopycnal mass fluxes were calculated by summing (4) over each season separately. Seasons are chosen so that winter is from

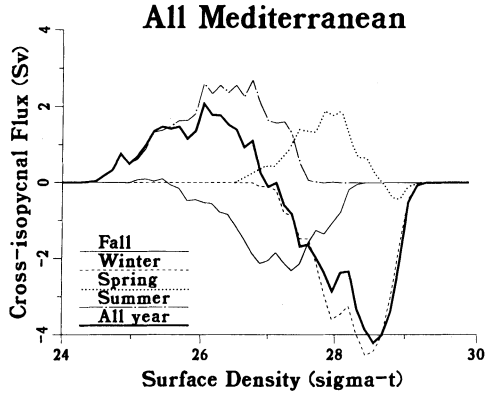

Fig. 1. Cross-isopycnal mass flux as function of the surface density, calculated for the whole Mediterranean Sea. The total flux calculated is divided by a time interval of 1 year and is shown in units of Sv (10^6 m^3 s^{-1}). The horizontal axis shows the density of the surface water for which the cross-isopycnal flux is calculated; sigma units are used for the density. The five lines shown are for the total flux calculated for the whole year (thick continuous line), and for the flux calculated for each of the four seasons: winter (dash); spring (dot); summer (dash–dot); autumn (thin continuous line).

December to February, spring is from March to May, etc. In all figures, the vertical axis is of the total volume flux divided by 1 year, $F(\rho)/(\rho_0 \times 1 \text{ year})$, shown in units of Sverdrup (Sv, 10^6 m^3 s^{-1}). It should be noted that, by (3), a positive slope of the curve of the cross-isopycnal mass flux $F(\rho)$ indicates water mass formation at the density ρ, whereas a negative slope indicates a net loss of water mass owing to the air–sea fluxes.

Let us consider first the results for the whole Mediterranean shown in Fig. 1. The thick continuous line describes the cross-isopycnal mass flux calculated for a full climatological year. The general shape of the flux is sinusoidal with a maximum at about $\sigma = 26.2$, corresponding to an averaged flux of about 2 Sv flowing from

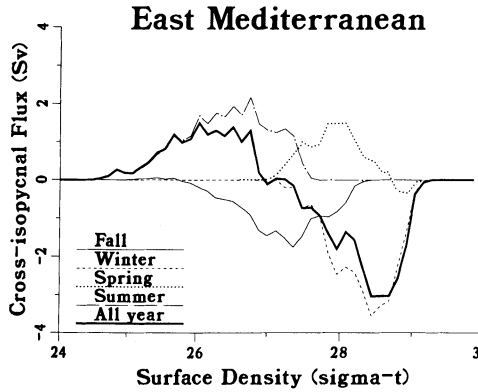

Fig. 2. As in Fig. 1, but for the East Mediterranean only, defined as the region east of 13°E.

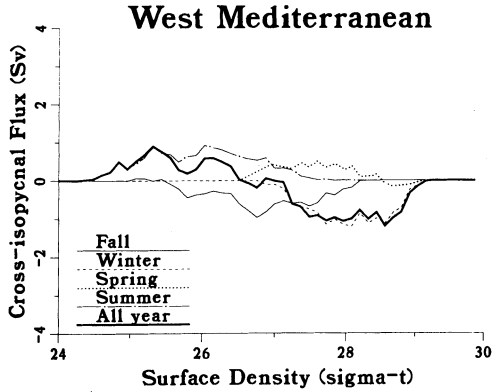

Fig. 3. As in Fig. 1, but for the West Mediterranean only, defined as the region west of 13°E.

greater densities to lower ones. The minimum flux is at about $\sigma = 28.7$, corresponding to about 4 Sv of light water transforming to greater densities. This means that during 1 year, the air–sea fluxes transform an average of 5–6 Sv of water from the density range $\sigma = (26.2, 28.7)$, to smaller and greater densities.

The temporal evolution of the water mass transformation can be studied from the seasonal curves of the cross-isopycnal mass flux in Fig. 1. During the winter season the cooling of surface water results in a transformation of about 4 Sv of water lighter than $\sigma = 28.5$ into denser water. (Note that the flux shown is the contribution of the flux during the winter season to the yearly averaged flux; i.e. it is the total flux during the winter season only, divided by a 1 year time period.) During the spring, the heating produces water of smaller densities, $\sigma = 26.5$–28. In the summer, there is a further transformation to less dense water. Finally, during the autumn, about the same amount of water that is transformed to lower densities

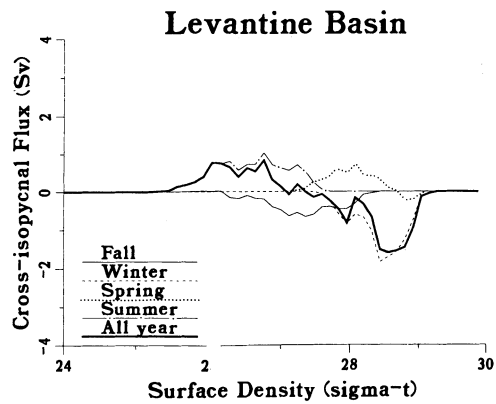

Fig. 4. As in Fig. 1, but for the Levantine basin of the East Mediterranean, defined as the region east of 25.5°E.

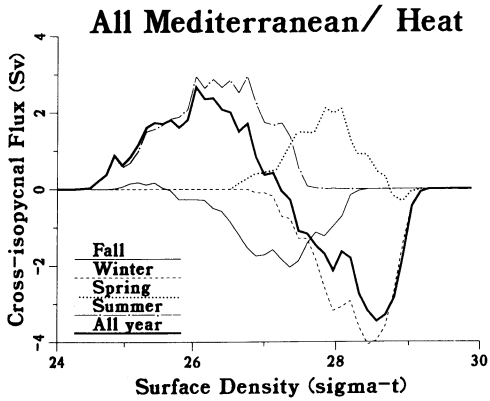

Fig. 5. As in Fig. 1, but only the contribution of air–sea heat fluxes to the water mass transformation curve $F(\rho)$ is calculated and shown, neglecting the contribution of evaporation and precipitation.

during the spring is made dense again. The effect of the transition seasons is qualitatively similar but opposite, such that they partially cancel each other. Their net effect is nevertheless to transfer water to the intermediate density range 27–28, thus reducing the steepness of the year-long average curve in this density range.

Figs. 2 and 3 show the transformation curves calculated for the East and West Mediterranean, with the 13°E longitude line separating the two parts. Fig. 4 shows the flux calculated for the Levantine basin only (east of 25.5°E), the site of Levantine Intermediate Water formation. The difference in magnitude of water mass transformation between the strong East Mediterranean transformation and the weaker West Mediterranean one should be noted.

Fig. 5 shows the water mass transformation flux $F(\rho)$ calculated for the entire

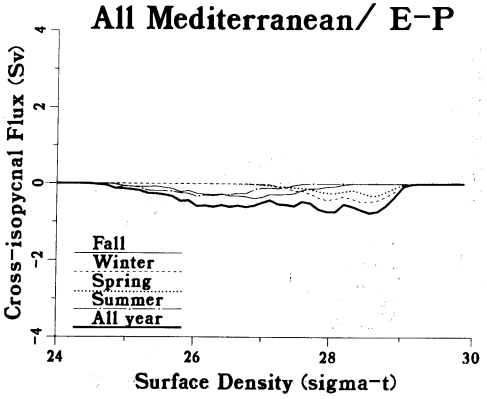

Fig. 6. As in Fig. 5, but showing only the contribution of evaporation and precipitation, and neglecting that of the air–sea heat fluxes.

Mediterranean, but using only the contribution of air–sea heat flux to (1), and Fig. 6 shows the contribution of the evaporation–precipitation alone. The strongest component of the annual average air–sea forcing of the thermohaline circulation in the Mediterranean seems to be the air–sea heat flux. The freshwater flux, which results in a net evaporation over the entire surface density range of the Mediterranean (Fig. 6), serves to remove buoyancy from all surface water masses, and therefore systematically enhances the water mass transformation towards dense and salty water masses. The amplitude of the water mass transformation owing to the freshwater flux alone is 0.5–0.75 Sv, close to the flux of the Gibraltar outflow and therefore is a key component of the contribution to the water mass transformation in the Mediterranean.

3.4. Discussion

3.4.1. Water mass formation

The water mass transformation curve $F(\rho)$ reflects the amount of dense water formed by air–sea fluxes at the surface. Some of this water sinks to form the deep water masses of the Mediterranean Sea (characterized by $\sigma > 29$), and some mixes with less dense water and remains near the surface. Our approach is incapable of distinguishing between dense water formation at the surface that results in shallow convection, and true deep water formation. It is of interest, however, to calculate the dense water formation at the surface owing to air–sea fluxes alone, as represented by $F(\rho)$. The amount of water formed at the surface with deep water properties is given by the value of the flux $F(\rho = 29)$, which, from Fig. 1, is about 1 Sv. This might be an underestimate, owing to the use of climatological data that have a lower surface density than the actual density during water mass formation events at extreme weather conditions (see the Appendix). It is possible, therefore, that the formation we calculate for water denser than $\sigma_\theta = 28.7$ (about 4 Sv) actually reflects the formation of water with deep water characteristics by air–sea fluxes at the surface. The result of 4 Sv is than probably a fairly loose bound on the amount of deep water (as opposed to surface water with deep water characteristics) formed by air–sea fluxes.

Bounds on the water mass formation rates for each of the different water masses of the Mediterranean Sea can be estimated by taking advantage of the geographically distinct formation sites of the deep water and the LIW. Fig. 4 shows $F(\rho)$ for the Levantine basin (east of Crete) only, where LIW is formed. The transformation $F(\rho)$ calculated for this region indicates that about 1.5 Sv (annual average) of surface water with LIW properties is formed in the East Mediterranean. Similarly, Fig. 2 gives about 1 Sv of dense water formation for the West Mediterranean. From Fig. 3, we deduce that 3 Sv of water formed in the East Mediterranean; subtracting the 1.5 Sv formed in the Levantine basin, this leaves about 1.5 Sv formed in the Ionian and Adriatic basins, presumably representing the formation of water with deep water properties at the surface of the Adriatic. Again, it should be noted that we cannot tell how much of this dense water sinks to form the observed deep waters.

3.4.2. Water mass budget, mixing

To maintain a steady stratification, the water mass formed or lost by each density range owing to the air–sea fluxes must be regained by the flow at Gibraltar, and the interior turbulent cross-isopycnal mixing. The inflow at Gibraltar is estimated to be about 1 Sv, at $\sigma_\theta = 26.8 \pm 0.3$, and the outflow has nearly the same transport, with $\sigma_\theta = 29.0 \pm 0.05$ (Kennelly et al., 1989).

The source at Gibraltar can be represented by a positive delta function of water mass formation, $M = \mathrm{d}F/\mathrm{d}\rho$, with unit height at $\sigma_\theta = 26.8$, and a negative delta function of unit height at $\sigma_\theta = 29$ (corresponding to 1 Sv of inflow and 1 Sv of outflow). To maintain a steady stratification, all sources of water at a given density need to balance (Tziperman, 1986):

$$M(\rho) + M_{\mathrm{G}}(\rho) + M_{\mathrm{M}}(\rho) = 0 \tag{5}$$

where subscript G corresponds to the Gibraltar source–sink and M to mixing. Integrating with respect to density gives

$$F(\rho) + F_{\mathrm{G}}(\rho) + F_{\mathrm{M}}(\rho) = 0 \tag{6}$$

The Gibraltar source is represented here as an equivalent cross-isopycnal flux F_{G} of a boxcar shape between σ_θ of 26.8 and 29, that is simply the integral of M_{G}.

The cross-isopycnal mass flux owing to mixing, F_{M}, can be calculated from (6), and a rough estimate of the interior cross-isopycnal velocity owing to mixing can be obtained (Walin, 1982), but this requires data from the interior as well as the surface. Although we cannot say where the mixing takes place from this analysis, some must be occurring at the surface, and some as deep interior mixing. The latter maintains the deep stratification by removing the dense and light water formed by the air–sea fluxes, and by forming water in the intermediate density range that is removed by the air–sea fluxes. A more detailed discussion of the mixing processes is left to the box model study of the following section, where a quantitative analysis of the mixing effects can be made.

It is interesting that the cross-isopycnal transports forced by the air–sea fluxes (4 Sv) are large compared with those required by a steady state with the inflow and outflow (1 Sv). This misfit between the vertical circulation required to balance the inflow and outflow at Gibraltar and the water mass transformation owing to air–sea fluxes is an indication of the strength of mixing in the Mediterranean Sea.

3.4.3. Seasonal effects on water mass transformation

The strong seasonality of the Mediterranean air–sea fluxes (reflected in the seasonality of $F(\rho)$) affects the transformation of the light Gibraltar inflow water to dense outflow water. Curiously, the inflow occurs at a density where the yearly averaged flux $F(\rho)$ is positive, and at about its maximum value. The sense of the cross-isopycnal mass flux implies that water of a density equal to the inflow density is, on average, made lighter and not denser by the air–sea fluxes. The water entering from Gibraltar during autumn and winter cooling is immediately converted to greater density, whereas during the spring and summer the inflow water is first made less dense by these air–sea fluxes. The inflow water entering during

the summer and spring can be made denser by mixing, to reach the density range where $F(\rho)$ is negative, where the water is dense enough to be turned into deep water by winter-time cooling and evaporation. The intuitive circulation cell in which Atlantic water continuously enters the Mediterranean, is subsequently made dense by surface fluxes, and then leaves the Mediterranean, is modified in the cycle forced by strong seasonal variations and mixing.

4. Box models of water mass transformation in a seasonally forced marginal sea

The analysis of the previous sections concentrated on the effects of air–sea fluxes on the water mass balance in the Mediterranean mostly disregarding mixing mechanisms because they cannot be identified from the data. To understand how the interplay between air–sea fluxes, mixing and the inflow–outflow determines the water mass transformation curves $F(\rho)$, we now use a simple three-box model of a marginal sea under seasonal forcing. This model is not meant to be realistic, yet it provides a useful qualitative description of water mass transformation within a marginal sea such as one of the basins within the Mediterranean Sea (e.g. the Levantine basin). The basin is assumed to be connected through an inflow–outflow to an adjacent ocean, and to contain deep water formation regions. The three-box model contains the effects of heat fluxes, evaporation minus precipitation, inflow and outflow, mixing and deep water formation.

We begin by analyzing a simpler one-box model of a mixed layer under seasonal heat fluxes with and without mixing, to demonstrate that mixing must be invoked to explain the shape of the water mass transformation curve calculated from the data.

4.1. Is mixing necessary to explain $\mathrm{F}_{air-sea}(\rho)$*? A one-box model*

The common view of the thermohaline circulation of the Mediterranean Sea is of the entering inflow water being made saltier and denser by the evaporation, and leaving as the outflow water. Mixing and air–sea heat fluxes are neglected in this picture. The latter are thought to heat and cool the surface water seasonally, but not produce yearly averaged water mass transformation. We now wish to demonstrate that this view of the insignificance of the mixing and air–sea fluxes is inconsistent with the results of the data analysis presented above, and that in the presence of mixing the air–sea heat fluxes do produce a net yearly transformation of mid-density water to the light and dense waters.

Let us consider a single-box model of a mixed layer exposed to seasonal heat fluxes, and subjected to mixing with an infinite heat reservoir below (i.e. a very deep lower layer). This model completely ignores the effects of the inflow and outflow, the deep water formation owing to unstable density profile and the effects of salinity and $(E-P)$.

Let the temperature of the mixed layer be denoted $T(t)$; the seasonal heat flux at the surface is simply $H(t) = -H_0 \cos(2\pi t/\tau)$; $\tau = 1$ year; the temperature of

the deep layer below the mixed layer is assumed constant and is denoted by T_{deep}; the mixing between the mixed layer and the deeper layer is determined by a mixing coefficient κ; d is the depth of the mixed layer and A its area. With this notation, the heat balance of the mixed layer may be written as

$$AdC_p\rho_0\frac{\partial T}{\partial t} = -AH_0\cos(2\pi t/\tau) + AC_p\rho_0\kappa(T_{\text{deep}} - T) \tag{7}$$

The solution for the mixed layer temperature is therefore

$$T(t) = T_{\text{deep}} + a\cos(2\pi t/\tau) + b\sin(2\pi t/\tau) \tag{8}$$

where

$$b = \frac{-\tau H_0}{2\pi dC_p\rho_0}\left[1 + \left(\frac{\kappa\tau}{2\pi d}\right)^2\right]^{-1}$$

$$a = \left(\frac{\kappa\tau}{2\pi d}\right)b \tag{9}$$

Let us consider first the two limits of this solution under weak and strong diffusion. For weak diffusion we find that the mixed layer temperature is nearly 90° out of phase from the surface heat flux:

$$T(t) \approx T_{\text{deep}} + \frac{-\tau H_0}{2\pi dC_p\rho_0}\sin(2\pi t/\tau); \qquad \frac{\kappa\tau}{2\pi d} \ll 1 \tag{10}$$

whereas for strong diffusion, the temperature and heat fluxes are in phase with each other:

$$T(t) \approx T_{\text{deep}} + \frac{-H_0}{\kappa C_p\rho_0}\cos(2\pi t/\tau); \qquad \frac{\kappa\tau}{2\pi d} \gg 1 \tag{11}$$

The heat flux and mixed layer temperature calculated from the solution (Eqs. (8) and (9)) and corresponding to a no-mixing case ($\kappa\tau/2\pi d = 0$) are shown in Fig. 7(a). The corresponding $F_{\text{air-sea}}(\rho)$ is shown in Fig. 7(b). Without mixing, the air–sea fluxes result in oscillations of the mixed layer density, leaving the net annual transformation to be zero. The seasonal components of the transformation do not vanish but rather cancel each other. Fig. 7(a) shows that each density is encountered twice during the year, where the heat flux at these times is equal but opposite, so that the net heat flux as a function of density vanishes for all densities.

In the presence of mixing ($\kappa\tau/2\pi d = 1$; Fig. 8), the mixed layer temperature is correlated with the air–sea heating, and the net heat flux for a given density does not vanish, leaving a net annually averaged transformation $F(\rho)$ that is qualitatively similar to that calculated from the data. The yearly transformation curve is positive for the light water and negative for the denser water. Mixing and seasonal heat fluxes are clearly crucial to the observed shape of the annually averaged transformation $F(\rho)$.

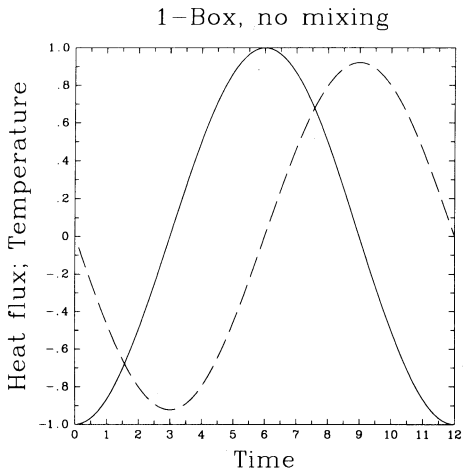

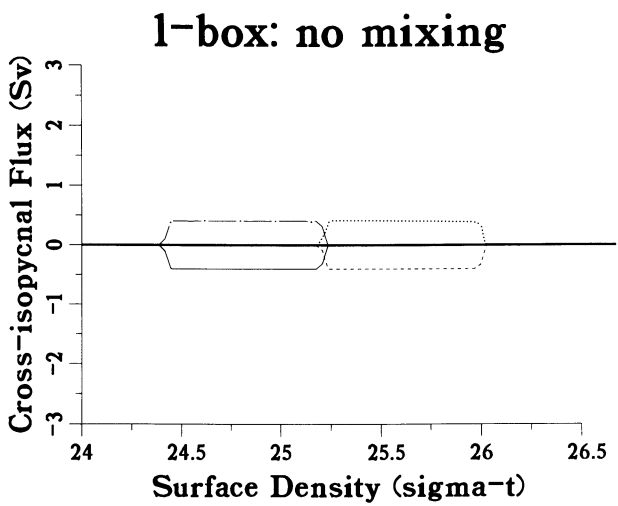

Fig. 7. (a) Seasonal evolution of air–sea heat flux (continuous line) and mixed layer temperature (dash line) (both in nondimensional units) for the one-box mixed layer model of Section 4.1 for a case of no mixing. (b) The water mass transformation $F(\rho)$ for this solution, including seasonal and yearly averaged curves.

4.2. The three-box model

The three-box model is schematically drawn in Fig. 9. The upper box represents the surface mixed layer water in the upper 25 m or so, which is directly affected by air–sea fluxes of heat and evaporation minus precipitation. The inflow water from the adjacent ocean enters the middle box, which represents the relatively fresh Atlantic Water (AW) mass lying in the Levantine basin between about 25 and 75 m depth. The lower box represents the Levantine Intermediate Water (LIW), from

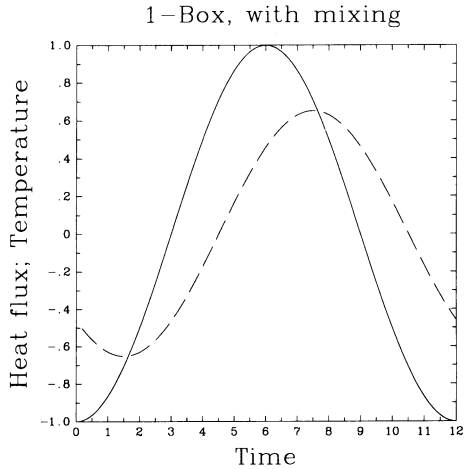

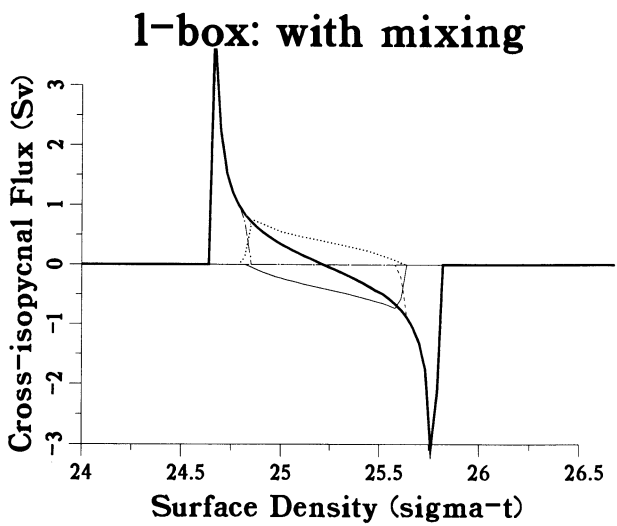

Fig. 8. As in Fig. 7, for non-vanishing mixing between the mixed layer and the deeper layer.

which the outflow to the adjacent ocean or basin occurs, and which lies between about 75 and 400 m in the Levantine basin.

The surface box variables are denoted by a subscript s, the middle box is denoted Box 1 and the lower box is denoted Box 2. The volume of the mixed layer surface box, V_s, is fixed in the model, yet the volumes of the two lower boxes are allowed to vary during the seasonal cycle. The variable volumes of the boxes allow the volume of the warm water box to increase owing to the inflow during the summer, and decrease again during the winter water mass formation events. The lower box volume reduces as it loses water to the outflow during the summer, and increases as it regains this water through winter water mass formation.

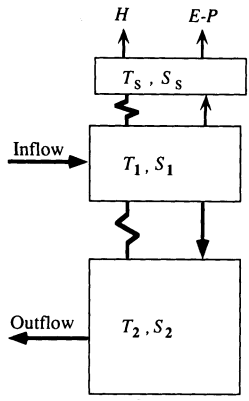

Fig. 9. A schematic drawing of the three-box model.

The inflow (M_I) is assumed constant; its temperature (T_I) varies seasonally, and the inflow salinity (S_I) is fixed. The surface fluxes of heat (H) and freshwater ($E-P$) affecting the upper box are also specified to vary seasonally such that there is net cooling and net evaporation during the year:

$$H(t) = \begin{cases} -H_0 \cos(2\pi t/\text{year}) & \text{when } H(t) > 0, \\ -1.3 \times H_0 \cos(2\pi t/\text{year}) & \text{when } H(t) < 0 \end{cases}$$

$$[E-P](t) = [E-P]_0 - \Delta[E-P] \sin(2\pi t/\text{year})$$

$$T_I = \bar{T}_I - \Delta T_I \sin(2\pi t/\text{year}); \qquad S_I = \bar{S}_I \tag{12}$$

The two upper boxes are linked by mixing that is proportional to the difference in temperature (and salinity) between the two boxes, with a mixing coefficient κ_s. The strong mixing that takes place during deep convection events, when the upper box density increases to that of the middle box, is parameterized by making the vertical diffusion coefficient much larger when the density profile is unstable or neutrally stable:

$$\kappa_s = \begin{cases} \kappa_{\text{convection}} & \text{if } \rho_s \geq \rho_1 \\ \kappa_{s;\text{background}} & \text{if } \rho_s < \rho 1, \end{cases} \tag{13}$$

where $\kappa_{\text{convection}} \gg \kappa_{s;\text{background}}$. To compensate for the loss of surface box water to the evaporation and maintain the box volume fixed, there is also a small flow of water from the middle to upper boxes, exactly balancing $(E-P)$.

The lower two boxes are also linked by vertical mixing, using a mixing coefficient κ,

$$\kappa = \begin{cases} \kappa_{\text{convection}} & \text{if } \rho_1 \geq \rho_2 \\ \kappa_{\text{background}} & \text{if } \rho_1 < \rho_2. \end{cases} \tag{14}$$

In addition, during the convection events there is a flow of middle box water to the

lower one, denoted M_{DC}, and parameterized in terms of the volumes of the two lower boxes

$$M_{DC} = \begin{cases} \Gamma M_I \exp\left[\left(\dfrac{V_1/\bar{V}_1}{V_2/\bar{V}_2} - 1\right)/\Delta\right] & \text{if } \rho_1 \geq \rho_2 \\ 0 & \text{if } \rho_1 < \rho_2 \end{cases} \tag{15}$$

The exponential feedback between the box volumes and the deep convection flow insures that the box volumes do not deviate too far from their specified average values, $\bar{V}_1 = Ad_1$ and $\bar{V}_2 = Ad_2$. This parameterization, although highly artificial, was found to produce reasonable results for our simple model and serves the purposes of this study.

The outflow from the lower box, M_O, is assumed to be constant throughout the year, and is set to the sum of the inflow and the averaged evaporation minus precipitation, to satisfy mass conservation:

$$M_O = M_I + \overline{(E-P)}A \tag{16}$$

where A denotes the area of the marginal sea. The evolution of the box volumes is given by the continuity equations

$$\frac{\partial V_s}{\partial t} = 0 \tag{17}$$

$$\frac{\partial V_1}{\partial t} = M_I - M_{DC} - A(E-P) \tag{18}$$

$$\frac{\partial V_2}{\partial t} = M_{DC} - M_O \tag{19}$$

The model equations for the temperature and salinity of the three boxes are

$$\frac{\partial V_s T_s}{\partial t} = A\kappa_s(T_1 - T_s)/\Delta z_s - A(E-P)(T_s - T_1) + \frac{A}{\rho_0 C_p}H(t) \tag{20}$$

$$\frac{\partial V_1 T_1}{\partial t} = A\kappa_s(T_s - T_1)/\Delta z_s + A\kappa(T_2 - T_1)/\Delta z + [M_I T_I - M_{DC} T_1 - A(E-P)T_1] \tag{21}$$

$$\frac{\partial V_2 T_2}{\partial t} = A\kappa(T_1 - T_2)/\Delta z + (M_{DC} T_1 - M_O T_2) \tag{22}$$

$$\frac{\partial V_s S_s}{\partial t} = A\kappa_s(S_1 - S_s)/\Delta z_s + A(E-P)(S_1) \tag{23}$$

$$\frac{\partial V_1 S_1}{\partial t} = A\kappa_s(S_s - S_1)/\Delta z_s + A\kappa(S_2 - S_1)/\Delta z - A(E-P)(S_1) + (M_I S_I - M_{DC} S_1) \tag{24}$$

$$\frac{\partial V_2 S_2}{\partial t} = A\kappa(S_1 - S_2)/\Delta z + (M_{DC} S_1 - M_O S_2) \tag{25}$$

where C_p is the specific heat of seawater; ρ_0 is a constant reference density; $\Delta z = (d_s + d_1)/2$ and $\Delta z = (d_1 + d_2)/2$ are the distances between the centers of the boxes.

These equations are solved by time stepping, using a 'leap-frog' time step, and at every time step the static stability of the model is examined to determine the occurrence of deep convection. The density is calculated using a simple linear equation of state,

$$\rho = \rho_0 - \alpha(T - 10) + \beta(S - 35) \tag{26}$$

For the runs presented below, the model parameters are chosen as follows: $\overline{T}_I = 19°$, $\Delta T_I = 2°$, $\overline{S}_I = 36‰$, $H_0 = 150$ Wm^{-2}, $(E-P)_0 = 80$ cm year^{-1}, $\Delta(E-P) = 60$ cm year^{-1}, $\rho_0 = 1$ gcm^{-3}, $\alpha = -1668. \times 10^{-4}$ gcm^{-3}°C^{-1}, $\beta = 0.781$ gcm^{-3}‰$^{-1}$, $\Gamma = 12$, $d_s = 25$ m, $d_1 = 50$ m, $d_2 = 500$ m, $A = 0.5 \times 10^{12}$ m^2, $\kappa_{s;\text{background}} = 0.2 \times 10^{-4}$ m^{2}s^{-1}, $\kappa_{\text{background}} = 0.1 \times 10^{-4}$ m^{2}s^{-1}, $\kappa_{\text{convection}} = 1000 \times 10^{-4}$ m^{2}s^{-1}.

The model is first run for about 1000 years under seasonal forcing conditions, until all transients are damped and the solution settles on a purely seasonal state. The results from a single year can then be used to calculate the water mass transformation in each box. Unlike the data analysis, all physical processes are precisely known now, and we can calculate the water mass formation owing to mixing, inflow and outflow.

4.3. Water mass transformation in the box model

We now derive the expressions for the water mass transformation owing to the different physical processes acting in the model, directly from the box model equations. The transformation is expressed as a function of the density of the water that is transformed, just as in the preceding data analysis. The results of this derivation are given by Eqs. (34)–(36) and the discussion following these equations. Readers interested mostly in the model results may skip to either these equations or the following two subsections where the specific model results are plotted and discussed.

Multiplying the temperature equation for each box (Eqs. (20)–(22)) by $-\alpha$, that of the salinity (Eqs. (23)–(25)) by β, adding them, and using the equations of state (Eq. (26)) and continuity (Eqs. (17)–(19)), we obtain

$$V_s = -\frac{A\alpha}{\rho_0 C_p}\frac{H}{\partial\rho_s/\partial t} + A(\rho_1 - \rho_s + \beta S_s)\frac{(E-P)}{\partial\rho_s/\partial t} + \frac{A\kappa_s}{\Delta z_s}\frac{(\rho_1 - \rho_s)}{\partial\rho_s/\partial t}$$

$$V_1(t) = \frac{M_I}{\partial\rho_1/\partial t}(\rho_1 - \rho_1) + \frac{A\kappa_s}{\Delta z_s}\frac{(\rho_s - \rho_1)}{\partial\rho_1/\partial t} + \frac{A\kappa}{\Delta z}\frac{(\rho_2 - \rho_1)}{\partial\rho_1/\partial t}$$

$$V_2(t) = \frac{A\kappa}{\Delta z}\frac{(\rho_1 - \rho_2)}{\partial\rho_2/\partial t} + M_{DC}\frac{(\rho_1 - \rho_2)}{\partial\rho_2/\partial t} \tag{27}$$

To convert the air–sea fluxes to be functions of the density of the upper box that is subjected to these fluxes, rather than functions of time, we divide by $|\partial\rho_s/\partial t|$ and integrate over the entire year by sampling only the instances $t = t'$ when the upper box density is equal to ρ'_s, to obtain, for example,

$$\frac{1}{\text{year}}\int_{1\text{ year}} \frac{H(t)}{|\partial\rho_s/\partial t|}\delta(t-t')\mathrm{d}t \equiv H(\rho'_s) \tag{28}$$

The various inflow, outflow and mixing terms are also written as function of the density in a similar way, e.g. for the mixing of the upper two boxes as function of the upper box density we have

$$\frac{1}{\text{year}}\int_{1\text{ year}} -\frac{A\kappa_s}{\Delta z_s}\frac{(\rho_1-\rho_s)}{|\partial\rho_s/\partial t|}\delta(t-t')\mathrm{d}t \equiv F^{s\leftrightarrow 1}_{\text{mixing}}(\rho'_s) \tag{29}$$

where t' represents the times when the upper box density, ρ is equal to ρ'_s. Similar expressions are used for the mixing of the lower two boxes. In all cases the mixing terms are written as a function of the density at which the water mass transformation is calculated.

Translating the continuity equations (Eqs. (17)–(19)) from time to density coordinates, using

$$\partial V_i/\partial t = (\partial\rho_i/\partial t)(\partial V_i/\partial\rho_i) \tag{30}$$

and combining them with the last set of equations for V_s, V_1 and V_2, we obtain

$$\frac{\partial}{\partial\rho_s}\left(-\frac{A\alpha}{\rho_0 C_p}H(\rho_s) + A(\rho_1-\rho_s+\beta S_s)(E-P)(\rho_s) - F^{s\leftrightarrow 1}_{\text{mixing}}(\rho'_s)\right) = 0 \tag{31}$$

$$\frac{\partial}{\partial\rho_1}\left[M_{\text{I}}(\rho_1)(\rho_{\text{I}}-\rho_1) + F^{s\leftrightarrow 1}_{\text{mixing}}(\rho_1) - F^{1\leftrightarrow 2}_{\text{mixing}}(\rho_1)\right]$$
$$= M_{\text{I}}(\rho_1) - M_{\text{DC}}(\rho_1) - A(E-P)(\rho_1) \tag{32}$$

$$\frac{\partial}{\partial\rho_2}\left[F^{1\leftrightarrow 2}_{\text{mixing}}(\rho_2) + (\rho_1-\rho_2)M_{\text{DC}}(\rho_2)\right] = -M_{\text{O}}(\rho_2) + M_{\text{DC}}(\rho_2) \tag{33}$$

The various terms in these equations represent the water mass formation and dissipation occurring in each of the boxes owing to the different physical processes acting there. The equations as a whole represent the condition that the total water mass formation, for each box and at any given density, vanishes to leave the yearly averaged water mass census for the box unchanged (compare with (2.13) and (2.23) of Tziperman (1986)). Integrating (31)–(33) once with respect to the density, we obtain

$$-\frac{A\alpha}{\rho_0 C_p}H(\rho_s) + A(\rho_1-\rho_s+\beta S_s)(E-P)(\rho_s) - F^{s\leftrightarrow 1}_{\text{mixing}}(\rho_s) = 0 \tag{34}$$

$$M_{\text{I}}(\rho_1)(\rho_{\text{I}}-\rho_1) - F^{s\leftrightarrow 1}_{\text{mixing}}(\rho_1) - F^{1\leftrightarrow 2}_{\text{mixing}}(\rho_1)$$

$$= \int_{\rho_{\min}}^{\rho_1} [M_I(\rho') - M_{DC}(\rho') - A(E-P)(\rho')] d\rho' \tag{35}$$

$$F^{1\leftrightarrow 2}_{\text{mixing}}(\rho_2) + M_{DC} \frac{(\rho_1 - \rho_2)}{\partial \rho_2 / \partial t} = \int_{\rho_{\min}}^{\rho_2} [-M_O(\rho') + M_{DC}(\rho')] d\rho' \tag{36}$$

Each term in these equations represents a mass flux from small densities to large ones, across a given density value, resulting from a specific physical process (mixing, air–sea fluxes, inflow and outflow). In the following subsection the various terms in Eqs. (34)–(36) are plotted, using the model solution for the temperature, salinity and density in all boxes.

4.4. Three-box model results

Using the model described above we solve for the seasonal cycle of temperature, salinity, density and box volume for all model boxes. We consider first the solution for the seasonal cycle of temperature, salinity and density of all boxes presented in Figs. 10(a)–10(c). Near the end of February, deep convection occurs in the model, and the temperature, salinity and density of all boxes are uniformly mixed. As spring warming begins, the stratification begins to build up again, and the upper box temperature increases. At the same time, the entering cool inflow water cools the middle box, so its temperature is decreased slightly. The stratification between the two lower boxes is stable now owing to the freshening effect of the inflow water. In May, the mixing between the upper and middle boxes starts heating the middle box, and its temperature increases. The autumn and winter cooling makes the density of the upper box equal to that of the middle box, and shallow convection starts between these boxes in November. From that time, and until the spring warming, the strong mixing between the two upper boxes (owing to the unstable vertical density gradient) keeps their properties equal. This strong mixing between the two upper boxes is similar to the formation of a deep mixed layer in the East Mediterranean during the winter. The density of the upper two boxes increases until it is equal to that of the lower box, at which point deep convection occurs throughout the depth of the water column, and deep water convection (M_{DC}) transfers water from the middle to the lower layer. This process stops again during the spring warming, and so on.

The box volumes and deep convection mass transfer from the middle to the lower boxes are shown in Fig. 10(d). The volume of the middle box increases owing to the inflow throughout the year, when $M_{DC} = 0$, and decreases during the short water mass formation event at the end of February when $M_{DC} > 0$.

The above description of the seasonal cycle in the model solution shows that the model provides a reasonable description of the evolution of a seasonally forced marginal sea. We now use the expressions derived in the previous subsection to analyze the water mass transformation in this model.

The quantities plotted in the data analysis of the previous sections are the water

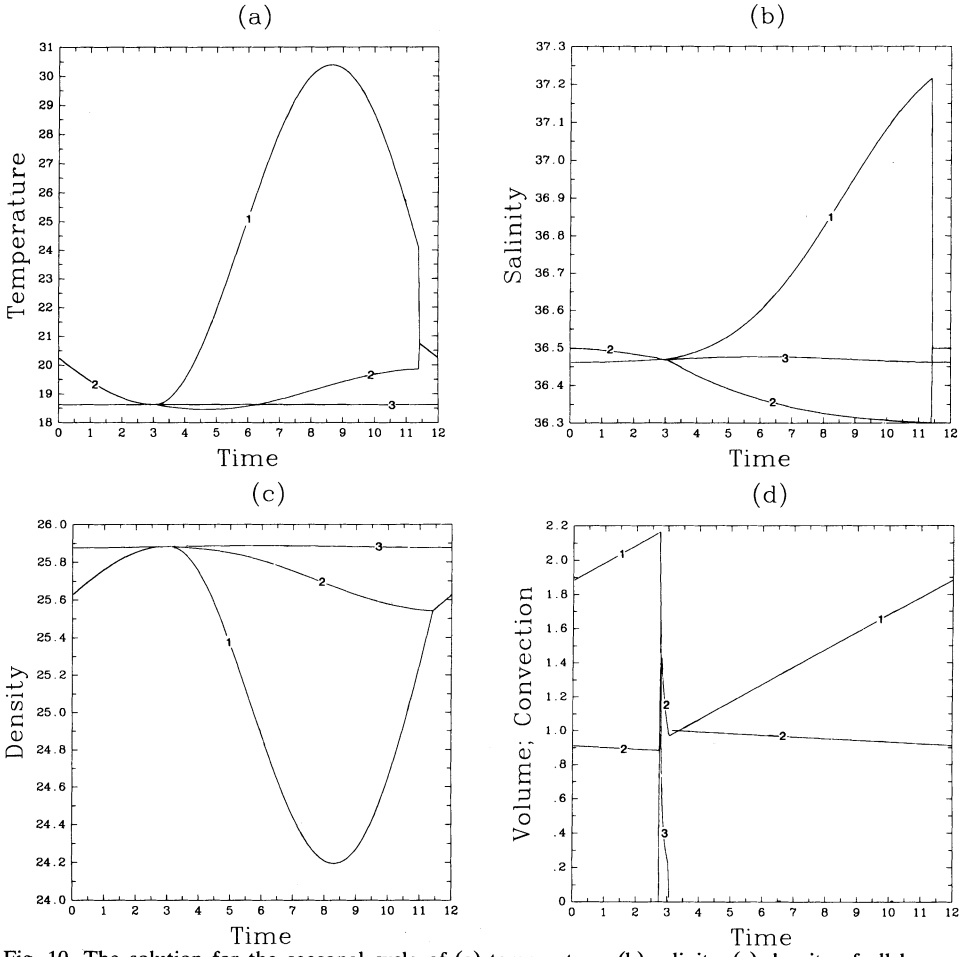

Fig. 10. The solution for the seasonal cycle of (a) temperature, (b) salinity, (c) density of all boxes. Shown as function of time for 1 year, with numbers on the horizontal axis denoting months. (d) The solution for the seasonal cycle of the box volumes and deep convection flow (MDC) from the middle box to the lower box.

mass transformation owing to the air–sea fluxes, i.e.

$$F_{\text{air-sea}}(\rho_s) = \frac{A\alpha}{\rho_0 C_p} H(\rho_s) - A(\beta S_s)(E-P)(\rho_s) \tag{37}$$

We are especially interested in the relation between the water mass transformations owing to the air–sea fluxes and the deep water formation as seen in the water mass transformation curves for the regime of highest densities. The interplay of

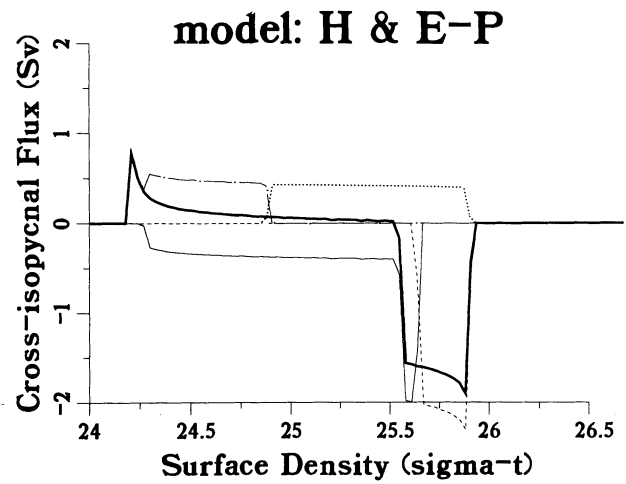

Fig. 11. The upper box water mass transformation curve owing to air–sea fluxes. Both yearly total and seasonal components are shown (see caption for Fig. 1; note that the results for both the yearly averaged transformation curves and the seasonal components are in excellent qualitative agreement with the results of the calculation using climatological data for the Mediterranean Sea (Fig. 1)).

mixing and the air–sea fluxes, responsible for shaping the water mass transformation curve at low densities, is also of interest.

The equation for the water mass transformation in the upper box (34) requires that, over a complete seasonal cycle, the total water mass transformation across a given density ρ_s owing to mixing and air–sea fluxes must exactly balance. We rewrite the no-net-flux condition for the upper box as follows:

$$F_{\text{air-sea}}(\rho_s) + F^{s\leftrightarrow 1}_{\text{mixing}}(\rho_s) - A(\rho_1 - \rho_s)(E-P)(\rho_s) = 0 \tag{38}$$

The first term on the left-hand side is the transformation owing to air–sea fluxes, and it is shown in Fig. 11 (both yearly total and seasonal components). The transformation is essentially proportional to the buoyancy flux experienced by the upper box owing to the air–sea fluxes. The buoyancy flux is positive during the summer when the surface density is low, and negative during the winter when the surface densities are high. This results in a water mass transformation curve owing to air–sea fluxes that is positive at low densities and negative at high densities, as we found from the data analysis. Even the different seasonal components in $F_{\text{air-sea}}(\rho)$ calculated from the model results are qualitatively similar to those calculated from the data (compare Figs. 1 and 11).

The transformation owing to mixing (Fig. 12) allows us to investigate specific mixing processes, as was not possible to do with the data analysis. At the low density range, the transformation curve is set during the summer season, when the density profile is stable. Thus the only mixing active there is the background mixing through $\kappa_{s;\text{background}}$. As the upper box density is lower than that of the middle box,

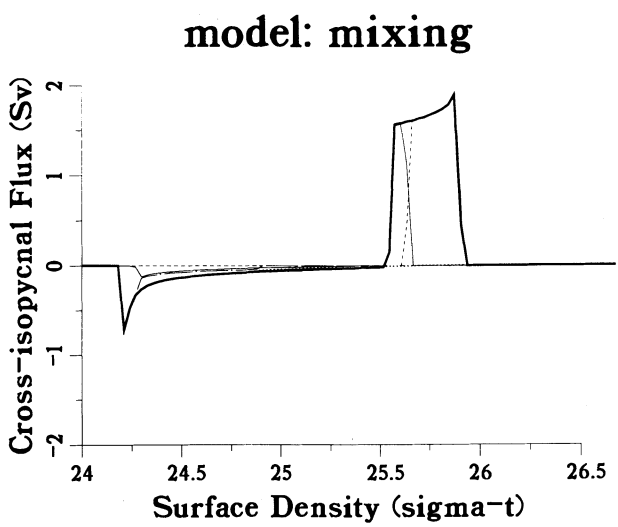

Fig. 12. The upper box water mass transformation curve owing to mixing with middle box (both yearly total and seasonal components).

the mixing term, proportional to $-(\rho_1 - \rho_s)$ is negative, balancing the positive contribution of the air–sea fluxes at this density range. In the higher density range, the dominant mixing term is the overturning parameterized by $\kappa_{\text{convection}}$. This mixing occurs when the upper box density is larger than or equal to that of the middle layer, thus its contribution to the transformation is positive, again balancing the air–sea fluxes at this density range. (It should be noted (Fig. 10) that the upper box density is never significantly larger than that of the middle box, because of the strong mixing when such an unstable profile exists.)

The water mass transformation in the surface water owing to the air–sea fluxes and the interior mixing (Figs. 11 and 12) dominate the surface box and nearly balance each other in the yearly average. The least important term in (38) is the contribution to the transformation owing to the small mass flux from the middle box to the upper one, balancing the mass lost to evaporation (not displayed). As the water entering from the middle box has different temperature and salinity, there is an implied mixing with the upper box water that brings the incoming water to the density of the upper box. This mixing affects the upper box, creating a small density change which is the source of this term.

The transformation in the middle box is influenced by several processes (35). The first term on the left-hand side is the implied mixing of the middle box water with the inflow water: the inflow water enters the middle box with different properties from those of the water in the middle box; the model assumes immediate mixing of the inflow water into the middle box, which implies a mixing that is proportional to the difference in the inflow and box water properties. This mixing is one of the dominant transformation mechanisms for this box. The next two

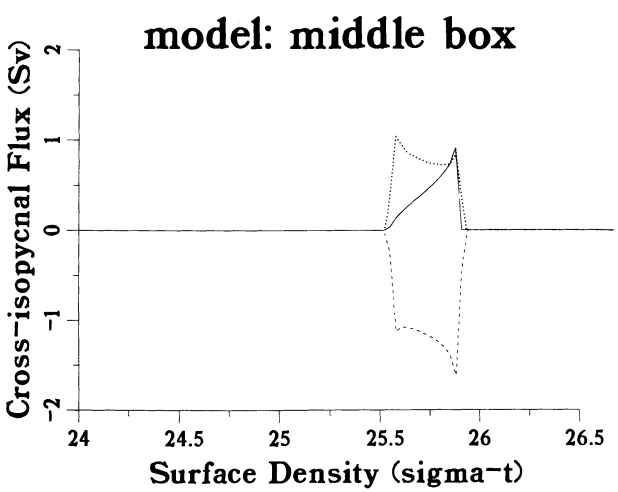

Fig. 13. Middle box yearly water mass transformation curves owing to mixing with upper layer (dash); mixing with the inflow water (dot) and the inflow–outflow (solid line).

terms in (35) represent the water mass transformation owing to mixing with the upper and lower boxes, including both background mixing when the stratification is stable and convective overturning mixing during deep water mass formation events. Finally, the right-hand side in (35) is the contribution of the mass sources and sinks owing to the inflow and outflow to the water mass transformation. This contribution is the integral over the inflow and mass losses as functions of the middle box density. This volumetric contribution of the inflow and mass losses is different from that owing to the mixing of the middle box with the inflow water.

The three main water mass transformation processes for the middle box are (Fig. 13) the mixing with the inflow water, the mixing with the upper layer containing the seasonal signal, and the contribution of the inflow and mass losses. The inflow occurs during the entire year, and therefore at the entire range of densities that occur in the middle box. This implies that the mass flux into water of density ρ_1, $M_I(\rho_1)$ has roughly a box-like shape. Accordingly, its integral with respect to the density, which gives its contribution to the water mass transformation in the middle box, gradually increases with density to a maximum value. The mass transfer from the middle to the lower boxes, on the other hand, occurs only during the winter deep convection events, when the middle box density attains its highest value. Accordingly, M_{DC} has a delta-function shape. Its integral is therefore a Heavyside function, with a sign opposite to that of the inflow contribution. Added together, the inflow and outflow cancel at densities higher than the maximum middle box density. The result is the curve given in Fig. 13.

As seen in Fig. 13, the inflow–outflow volumetric contribution together with the mixing with the inflow water balance the transformation owing to the air–sea fluxes manifest through mixing with the upper layer. The mixing with the lower layer has a smaller and negligible contribution.

4.5. Discussion of box-model results

Using a two-box model in which the box exposed to air–sea fluxes is also the one into which the inflow occurs (not shown), we found that the air–sea transformation curve has a very different form from that found from the climatological Mediterranean data. It seems that the 'lateral' mixing with the inflow water implied in the box model is a dominant mechanism that strongly affects the properties of the box into which the inflow occurs, and therefore affects the water mass transformation curves. For the model transformation curve to have the characteristic shape as found from the data, the water exposed to the air–sea fluxes should be only weakly coupled to the box with the inflow water. This weak coupling occurs through the mixing between the upper and middle boxes. On the one hand this mixing needs to be weak to allow reasonable surface temperature excursions, but on the other hand it is crucial to drive the convection to lower layers. Both the single-box model and the three-box model show that the mixing processes are responsible for shaping the air–sea flux transformation curve.

Next, we consider the relation between the air–sea transformation curve (37) and the water mass formation rates. While analyzing the climatological flux data, we suggested that the value of this curve at high densities provides an upper bound for the amount of deep water formation. Fig. 11 shows that the transformation owing to air–sea fluxes at the highest density is about 1.9 Sv. The deep water formation (flow from the middle to lower boxes) is specified in the model to be 1 Sv, which is indeed less than the bound calculated from $F_{\text{air-sea}}(\rho)$. Our very idealized model cannot indicate how tight the bounds are for the water mass formation obtained from the climatological data. In various model runs the ratio between the bound given by the air–sea fluxes transformation curve and the actual water mass formation varied from 1.5 to more than 10.

5. Conclusions

Using climatological air–sea fluxes and surface temperature and salinity, we estimated the amounts of water modified by the air–sea fluxes of heat and freshwater above the Mediterranean Sea. This was done by calculating the buoyancy flux as a function of the density of the surface water losing or gaining this flux ($F_{\text{air-sea}}(\rho)$), rather than as a function of location and time.

Approximate bounds on the water mass formation are obtained from this calculation. The total formation of dense water in the entire Mediterranean Sea is found to be no larger than 4 Sv on the average. Much of this dense water formation is balanced by the internal thermohaline circulation of the Mediterranean Sea, and only about 1 Sv is balanced by the Gibraltar outflow. The bounds on the formation of Levantine Intermediate Water, Adriatic deep water, and deep water of the west Mediterranean are about 1–1.5 Sv for each of these water

masses. The water mass transformation within the Mediterranean Sea is estimated to be much larger than needed to supply the 1 Sv circulation cell implied by the Gibraltar source alone.

Various aspects of the water mass transformation process that could not be quantified using the data were examined using a simple three-box model of a marginal sea under seasonal forcing. The model uses variable-volume boxes to demonstrate the importance of mixing to the water mass transformation process and to confirm the structure of both the seasonal and annual components of $F_{\text{air-sea}}(\rho)$ calculated from the data.

The picture of water mass transformation presented in this work is somewhat different from the more common view of the thermohaline circulation of the Mediterranean Sea. This circulation is often described as being composed of the entering inflow water being made saltier and denser by the evaporation, and leaving as the outflow water. In this picture, the air–sea heat fluxes only heat and cool the surface water, with no net water mass transformation occurring during the year. We have demonstrated that this view of the insignificance of the air–sea fluxes is inconsistent with the results of the data analysis, and that in the presence of mixing the air–sea heat fluxes produce net transformation of water from the mid-density range to the light and dense extremes of the density range. This transformation is balanced by an opposite transformation owing to the mixing processes that mix the extreme densities to form the mid-density water mass. The mixing mechanisms that were not possible to identify in the data analysis were explicitly examined in the box models study. It seems that a crucial factor determining the water mass transformation, $F_{\text{air-sea}}(\rho)$, is the mixing between the surface mixed layer and the deeper water (Atlantic Water) into which the inflow occurs. We also showed that it is equally crucial that the link between the mixed layer and the lower Atlantic Water would not be too strong for the water mass transformation to have its observed characteristics.

The air–sea flux data available for this calculation are, unfortunately, of insufficient quality for an accurate determination of water mass formation rates at high density resolution, but some useful results are nevertheless obtained even from these data. As better data of surface properties and air–sea fluxes become available, perhaps through the use of remote sensing methods, the simple analysis used here may prove very useful in a quantitative study of water mass transformation in the Mediterranean Sea and elsewhere.

Acknowledgments

We are grateful to the eight reviewers and three editors who have helped to perfect this work.

E.T. was supported by Grant 87-00385 from the United States–Israel Binational Science Foundation. K.S. was supported by the Bundesministerium für Forchungs und Technologie and the Centre National de la Recherche Scientifique. We wish to thank Paola Rizzoli (funded by NSF OCE-85-18487) for helping with the initial data analysis.

Appendix: analysis of sources of errors in $F(\rho)$

In this Appendix we examine and estimate possible sources of errors in our calculations. First, we apply our method to a different air–sea flux data set from that discussed in the text, to obtain a rough idea of the expected error owing to the known poor quality of the fluxes. Then, we examine the sensitivity of the results to the sampling interval used in the calculation of the water mass transformation $F(\rho)$. Finally, we discuss the errors caused by our data for the surface fluxes and properties being climatologically and monthly averaged, rather than instantaneous as required by the method we use. This Appendix indicates that the results presented in the text for the Mediterranean water mass transformation may be expected to be useful in spite of the fairly large uncertainties involved.

Errors in the climatological air–sea flux data

Bunker et al. (1982) calculated the total heat flux from the Mediterranean Sea, and compared it with the heat flux through the Straits of Gibraltar as estimated from oceanographic observations. They found an averaged gain of heat of 20–35 W m^{-2} by the Mediterranean, instead of a net loss to the atmosphere of 5 W m^{-2} expected from the Gibraltar outflow characteristics.

Our heat flux data set (May, 1983) is believed to be better than the Bunker et al. calculation. Still, after being interpolated to the half-degree grid, it gives a small averaged surplus of 5 W m^{-2} for the entire Mediterranean. We have adjusted the heat flux data by subtracting a constant value from all data points and at all months, to satisfy the integral constraint on the heat budget of the entire Mediterranean. As the integral imbalance is a result of an accumulating small error over all densities, it does not imply that the calculation of $F(\rho)$ is grossly biased at any particular density. The water mass transformation $F(\rho)$ is determined only by the heat gained or lost by surface water of density ρ, and is not sensitive to the small systematic errors that are responsible for the misfit of the integral heat budget to the expected total loss of heat by the Mediterranean Sea. The total freshwater balance calculated from our evaporation and precipitation data gives an average loss of 101 cm $year^{-1}$, in accordance with previous estimates, which range from 0.5 to 1.5 m $year^{-1}$.

Formal error bars are not available for the air–sea flux data used here. Instead, we estimate $F(\rho)$ from an independent data (Oberhuber, 1988) for the air–sea fluxes and sea surface temperature, while using the Levitus (1982) data for the sea surface salinity. The results for the yearly averaged transformation curve are given in Fig. A1, together with the results shown in the text of this paper, using our 'standard' data (i.e. the Jaeger (1976) and May (1983) data sets).

The overall buoyancy balance of the Mediterranean (the integral of $F(\rho)$) is clearly positive for the Oberhuber (1988) data, whereas it should be negative. The part of the $F(\rho)$ curve for the lower density range, $\sigma < 27$, is not in very good agreement with our previous results, although the difference is of the order of 30–50%, as expected from the air–sea flux error estimates. The results for $F(\rho)$

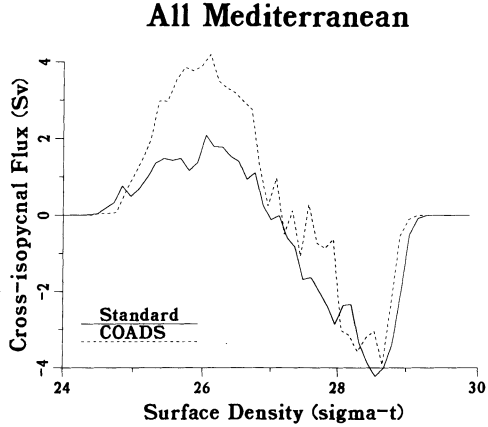

Fig. A1. Cross-isopycnal mass flux as function of the surface density, calculated for the whole Mediterranean Sea, using two different data sets for the air–sea flux data. (See Appendix for details.)

obtained from the two data sets for the upper density range ($\sigma > 27$), indicating dense water formation with properties of intermediate and deep water masses, are encouragingly similar.

Sensitivity of F(ρ) *to the density sampling interval* (Δρ)

We have calculated $F(\rho)$ for three choices of $\Delta\rho$ (see Section 3.2), and the results are presented in Fig. A2. Clearly, even the very different choices for the density sampling interval used in calculating the shown curves do not significantly affect our results for the water mass transformation. The choice of $\Delta\rho = 0.12$ is

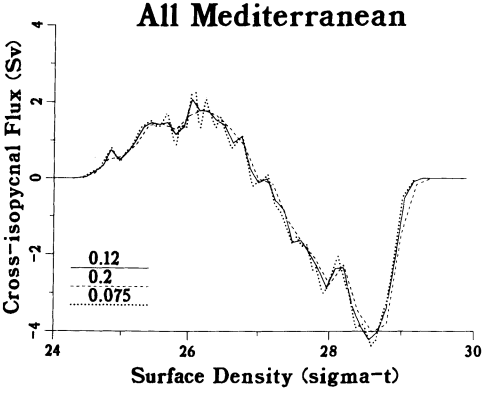

Fig. A2. Cross-isopycnal mass flux as function of the surface density, calculated for the whole Mediterranean Sea, using three different sampling intervals for the density ($\Delta\rho$): 0.12, 0.2 and 0.075 sigma units. (See Appendix for details.)

seen in Fig. A2 to be a reasonable compromise between high resolution (small $\Delta\rho$) and a resulting noisy curve, and low resolution (large $\Delta\rho$) with a smoother curve.

Errors in calculating $F(\rho)$ *from monthly climatological data*

Deep water mass formation is known to occur during short time intervals characterized by intense weather conditions that are obviously not found in the climatological averages (although they do contribute to these averages in principle). It is worth while, therefore, to try and quantify the errors in the cross-isopycnal flux $F(\rho)$ resulting from the use of climatological data.

We analyze only the contribution of the heat fluxes to the water mass transformation estimate, ignoring the freshwater flux that can be treated in a similar manner. We find that a calculation of water mass formation based on monthly averaged data may be expected to yield reasonable results in spite of the missing information on the instantaneous air–sea fluxes.

With perfect knowledge of the heat flux and surface density as function of space and time, over many years, the average cross-isopycnal flux can be written as

$$F(\rho') = \left\langle \int_{1 \text{ year}} dt \iint_{\text{surface area}} dx\,dy \left[\frac{\alpha}{C_p} \mathscr{H}(x,y,t) \right] \delta[\rho(x,y,t) - \rho'] \right\rangle, \tag{A1}$$

where $\langle\ \rangle$ indicate average over many years of data. In practice, only climatological estimates of the heat flux and surface density are normally known, with monthly resolution. Denoting the climatological monthly air–sea heat fluxes by $\overline{\mathscr{H}}^{\mathrm{m}}(x,y)$, its relation to the instantaneous air–sea fluxes, $\mathscr{H}(x,y,t)$, is

$$\overline{\mathscr{H}}^{\mathrm{m}}(x,y) = \left\langle \frac{1}{\text{month}} \int_{m\text{th month}} dt\, \mathscr{H}(x,y,t) \right\rangle, \quad m = 1,\ldots,12 \tag{A2}$$

The mass flux across an isopycnal ρ', estimated from monthly climatological data, can then be written as a sum of its monthly components,

$$\tilde{F}(\rho') = \sum_{1}^{12} \tilde{F}^{\mathrm{m}}(\rho')$$

where

$$\tilde{F}^{\mathrm{m}}(\rho') = \iint_{\text{surface area}} dx\,dy \left[\frac{\alpha}{C_p} \overline{\mathscr{H}}^{\mathrm{m}}(x,y) \right] \delta\left[\overline{\rho}^{\mathrm{m}}(x,y) - \rho' \right] \tag{A3}$$

The error in the climatological estimate $\tilde{F}(\rho')$ is therefore a sum over 12 months of the monthly error, which is in turn related to the difference between the instantaneous fluxes and their climatological monthly averages

$$\epsilon^{\mathrm{m}}(\rho') = \left\langle \int_{1 \text{ month}} dt \iint_{\text{surface area}} dx\, dy \frac{\alpha}{C_p} \left(\{ \mathscr{H}(x,y,t) \delta[\rho(x,y,t) - \rho'] \} \right.\right.$$
$$\left.\left. - \{ \overline{\mathscr{H}}^{\mathrm{m}}(x,y) \delta[\overline{\rho}^{\mathrm{m}}(x,y) - \rho'] \} \right) \right\rangle \tag{A4}$$

To understand this expression for the error, we decompose the heat flux during the mth month into a monthly averaged value, $\overline{\mathscr{H}}^{\mathrm{m}}(x,y)$, and a variable component, $\Delta\mathscr{H}(x,y,t)$, that may vary during the month, and between different years:

$$\mathscr{H}(x,y,t) = \overline{\mathscr{H}}^{\mathrm{m}}(x,y) + \Delta\mathscr{H}(x,y,t), \text{ where } \left\langle \int_{m\text{th month}} \mathrm{d}t \Delta\mathscr{H}(x,y,t) \right\rangle \equiv 0 \tag{A5}$$

Substituting (A5) into (A4), we have

$$\epsilon^{\mathrm{m}}(\rho') = \left\langle \int_{\text{m'th month}} \mathrm{d}t \iint_{\text{surface area}} \mathrm{d}x\,\mathrm{d}y \left(\frac{\alpha}{C_p} \mathscr{H}(x,y,t) \{ \delta[\rho(x,y,t) - \rho'] - \delta[\bar{\rho}^{\mathrm{m}}(x,y) - \rho'] \} \right) \right\rangle$$

$$+ \left\langle \int_{\text{m'th month}} \mathrm{d}t \iint_{\text{surface area}} \mathrm{d}x\,\mathrm{d}y \left(\frac{\alpha}{C_p} \{ \Delta\mathscr{H}(x,y,t) \delta[\bar{\rho}^{\mathrm{m}}(x,y) - \rho'] \} \right) \right\rangle$$

By its definition, the term linear in $\Delta\mathscr{H}$ vanishes under the many year averaging, leaving us with the final expression for the monthly error

$$\epsilon^{\mathrm{m}}(\rho') = \left\langle \int_{\text{m'th month}} \mathrm{d}t \iint_{\text{surface area}} \mathrm{d}x\,\mathrm{d}y \left(\frac{\alpha}{C_p} \mathscr{H}(x,y,t) \times \{ \delta[\rho(x,y,t) - \rho'] - \delta[\bar{\rho}^{\mathrm{m}}(x,y) - \rho'] \} \right) \right\rangle \tag{A6}$$

The possible source of error in the calculation of the water mass transformation flux $F(\rho)$ from climatological data is clearer now. It is due to the sampling of the heat fluxes where the climatological density $\bar{\rho}$ is equal to ρ' rather than where the instantaneous density ρ is equal to ρ'. As long as the variations of surface density at a given location during a given month are not too large, we may expect the calculation based on climatological averages to yield reasonable results. One may intuitively expect the errors in calculating $F(\rho)$ to result mostly from the inability of the climatological data to resolve the outbreaks of cooling during water mass formation events. However, the above calculation shows that this in fact is not a major problem, and that the errors result mostly from deviations of the surface density field from its monthly mean. Because the surface density is affected by the integral over time of the surface fluxes, its behavior is smoother in time, and its deviations from the monthly mean are probably much smaller than those of the air–sea heat fluxes.

References

Andersson, L., Rudels, B. and Walin, G., 1982. Computations of heat flux through the ocean surface as a function of temperature. Tellus, 34: 196–198.

Bunker, A.F. and Goldsmith, R.A., 1979. Archived time series of Atlantic Ocean meteorological variables and surface fluxes. Woods Hole Oceanographic Institution, Woods Hole, MA, Tech. Rep. WHOI 79-3, 28 pp.

Bunker, A.F., Charnock, H. and Goldsmith, R.A., 1982. A note on the heat balance of the Mediterranean and Red Seas. J. Mar. Res., 40(Suppl.): 73–84.

Davis, M.D., Countryman, K.A. and Carron, M.J., 1986. Tailored acoustic products utilizing the NAVOCEANO GDEM (a generalized digital environmental model). Naval Oceanographic Office, Bay St. Louis, Stennis Space Center, Mississippi, 24 pp.

Hopkins, T.S., 1988. Physics of the sea. In: Western Mediterranean, Key Environment Series. Pergamon, Oxford, pp. 100–125.

Jaeger, L., 1976. Monatskarten des Niederschlags fur die ganze Erde. Ber. Dtsch. Wetterdienstes, 18(139) (in German).

Lascaratos, A., 1993. Estimation of deep and intermediate water mass formation rates in the Mediterranean Sea. Deep-Sea Res., II, 40(6): 1327–1332.

Malanotte-Rizzoli, P. and Hecht, A., 1988. Large-scale properties of the eastern Mediterranean: a review. Oceanol. Acta, II(4): 323–335.

Kennelly, M.A., Sanford, T.B. and Lehman, T.W., 1989. CTD data from the Gulf of Cadiz Expedition: R.V. OCEANUS cruise 202. Tech. Rep. APL-UW TR 8917, Applied Physics Laboratory, University of Washington, Seattle.

Levitus, S., 1982. Climatological atlas of the world ocean. NOAA Tech. Pap., 3, 173 pp.

May, W.P., 1983. Climatological flux estimates in the Mediterranean Sea. Part II. Air–sea fluxes. Norda Rep. 58, 65 pp.

Oberhuber, J.M., 1988. An atlas based on the COADS data set: the budgets of heat, buoyancy and turbulent kinetic energy at the surface of the global ocean. Max-Planck Institut für Meteorologie, Rep. 15, Hamburg.

Speer, K. and Tziperman, E., 1992. Rates of water mass formation in the North Atlantic Ocean. J. Phys. Oceanogr., 22: 94–104.

Tziperman, E., 1986. On the role of interior mixing and air–sea fluxes in determining the stratification and circulation of the oceans. J. Phys. Oceanogr., 16: 680–693.

Walin, G., 1982. On the relation between sea-surface heat flow and the thermal circulation in the ocean. Tellus, 34: 187–195.

Wüst, G., 1960. On the vertical circulation of the Mediterranean Sea. J. Geophys. Res., 66: 3261–3271.

Note to Contributors

A detailed *Guide for Authors* is available upon your request, and is also printed in Volume 21 / 1, pp. 49–52. You are kindly asked to consult this guide. Please pay special attention to the following notes.

Language

The official language of the journal is English, but occasional articles in French or German will be considered for publication. Such articles should start with an abstract in English, headed by an English translation of the title. An abstract in the language of the paper should follow the English abstract. English translations of the figure captions should also be given.

Preparation of the text

a) The manuscript should include at the beginning of the paper an abstract of not more than 500 words. It should be typewritten with double spacing and wide margins. Words to be printed in italics should be underlined. The metric system should be used throughout.

b) The title page should include: the title, the name(s) of the author(s), and their affiliation.

References

a) References in the text start with the name of the author(s), followed by the year of publication in parentheses.

b) The reference list should be in alphabetical order and on sheets separate from the text.

Tables

Tables should be compiled on separate sheets. A title should be provided for each table and they should be referred to in the text.

Illustrations

a) All illustrations should be numbered consecutively and referred to in the text.

b) Drawings should be completely lettered, the size of the lettering being appropriate to that of the drawings, but taking into account the possible need for reduction in size (preferably not more than 50%). The page format of the journal should be considered in designing drawings.

c) Photographs must be of good quality, printed on glossy paper.

d) Figure captions should be supplied on a separate sheet.

Proofs

One set of proofs will be sent to the author to be checked for printer's errors. In the case of two or more authors please indicate to whom the proofs should be sent.

Reprints and page charges

There will be no page charge. Fifty reprints of each article published will be supplied free of charge. Additional reprints can be ordered on a reprint order form which is included with the proofs.

Submission of manuscripts

Two copies should be submitted to: Prof. A.R. Robinson, Division of Applied Sciences, Harvard University, Pierce Hall, Cambridge, MA 02138 (USA). One set of illustrations should be of good quality, the other may be of a lower quality.

Submission of an article is understood to imply that the article is original and unpublished and is not being considered for publication elsewhere.

Upon acceptance of an article by the journal, the author(s) will be asked to transfer the copyright of the article to the publisher. This transfer will ensure the widest possible dissemination of information under Copyright Law.

Submission of electronic text

In order to publish the paper as quickly as possible after acceptance, authors are encouraged to submit the final text also on a 3.5" or 5.25" diskette. Both double density (DD) and high density (HD) diskettes are acceptable. Make sure, however, that the diskettes are formatted according to their capacity (HD or DD) before copying the files onto them. Similar to the requirements for manuscript submission, main text, list of references, tables and figure legends should be stored in separate text files with clearly identifiable file names. The format of these files depends on the word processor used. Texts made with DisplayWrite, MultiMate, Microsoft Word, Samna Word, Sprint, Volkswriter, Wang PC, WordMARC, WordPerfect, Wordstar, or supplied in DCA / RFT, or DEC / DX format can be readily processed. In all other cases the preferred format is DOS text or ASCII. It is essential that the name and version of the wordprocessing program, type of computer on which the text was prepared, and format of the text files are clearly indicated. Authors are encouraged to ensure that **the disk version and the hardcopy must be identical**. Discrepancies can lead to proofs of the wrong version being made.

0377-0265/94/$07.00

(∞) The paper used in this publication meets the requirements of ANSI/NISO 239.48-1992 (Permanence of Paper).

PRINTED IN THE NETHERLANDS